Ceramics-Silikáty 64 (3), 365-370 (2020)
www.ceramics-silikaty.cz doi: 10.13168/cs.2020.0024

FOAM-GELCASTING PREPARATION OF $ZrSiO_4$ MODIFIED POROUS MULLITE CERAMICS

XUEYIN LIU*, SHENGTAO GE**, #HAIJUN ZHANG**, YUBAO BI**, QUANLI JIA***, #SHAOWEI ZHANG****

*College of Civil Engineering and Architecture, Quzhou University, Quzhou 324000, China
**The State Key Laboratory of Refractories and Metallurgy, Wuhan University of Science and Technology, Wuhan 430081, China
***School of Materials Science and Engineering, Zhengzhou University, Zhengzhou 450002, China
****College of Engineering, Mathematics and Physical Sciences, University of Exeter, Exeter EX4 4QF, UK

#E-mail: zhanghaijun@wust.edu.cn (H. Zhang), s.zhang@exeter.ac.uk (S. Zhang)

Submitted February 9, 2020; accepted March 9, 2020

Keywords: Microstructure, Pore size distribution, Thermal conductivity, Mechanical property

$ZrSiO_4$ modified mullite-based porous ceramics were fabricated at 1400 °C by using a foam-gelcasting method from industrial grade powder materials. Except for mullite and $ZrSiO_4$ no other phases were identified in the fired samples added with $ZrSiO_4$, implying that at the firing temperature, $ZrSiO_4$ neither decomposed, nor reacted with mullite. In the microstructures of these samples, mullite/$ZrSiO_4$ grains were evenly distributed, and the overall pore sizes were reduced. The addition of $ZrSiO_4$ showed little effect on porosity and bulk density of fired samples, which were respectively around 77 % and 0.7 $g \cdot cm^{-3}$. However, it led to the enhanced mechanical strength, and more importantly, the reduced thermal conductivity, especially at high temperatures. When 8 wt. % $ZrSiO_4$ was added, flexural and compressive strengths increased respectively to 3.63 and 7.35 MPa, whereas thermal conductivity at 200 and 1000 °C was reduced to 0.160 and 0.277 $W \cdot m^{-1} \cdot K^{-1}$, respectively, which was mainly attributed to the shading effect, decreased size of "large" spherical pores, and more centralized and homogenized pore size distribution.

INTRODUCTION

Porous mullite ceramics are good insulation materials possessing superior properties like high melting (1850 °C), small thermal expansion, chemical inertness, lightweight and low thermal conductivity [1-4]. Various strategies/methodologies have been adopted to fabricate them, including sacrificial template [5, 6], gel/freeze casting [7, 8], particle stacking [9, 10], use of pore-former [11, 12] as well as foam-gelcasting [13, 14]. Compared with other techniques, the foam-gelcasting technique shows several advantages, for example, it is easy to operate, low cost, and scalable, and the resultant products exhibit excellent properties and performance [14, 15].

The thermal behaviour and performance of a porous insulation material has great effects on the energy efficiency, and is thus a critical issue concerning high temperature industries. Generally, the thermal conductivity of an insulation ceramic is higher at elevated temperature than at ambient temperature [16-20]. Considering the actual service condition, thermal conductivity examined at elevated temperature should be more meaningful than that examined at ambient temperature.

Heat is transferred in three complex modes: solid/gas conduction, natural convection, and heat radiation, and the relative contribution from each mode depends on the operation condition. With an increase in temperature, heat radiation in an insulation material becomes more and more significant, though it is almost negligible at room temperature [21]. The mechanism corresponding to this mode is complex, making it hard to analyze. Nevertheless, reduction of heat radiation is key in lowering thermal conductivity of a material, i.e., improving its insulation performance, at a high temperature.

Since heat radiation is the major contributor to the increased thermal conductivity at high temperatures, additives like $ZrSiO_4$ were introduced into a base material as an infrared (IR) opacifer [22, 23] for effectively blocking the IR radiation and reducing the thermal conductivity, providing an alternative approach to the improvement in thermal insulation of a composite material, especially in a demanding operational environment.

In this paper, to further enhance the insulation performance of mullite-based porous ceramics at high temperatures, $ZrSiO_4$ powder was added and investigated as an IR opacifier. A foam-gelcasting based technique was developed and used to prepare the desired highly porous $ZrSiO_4$ modified mullite ceramics. The influence of $ZrSiO_4$ addition on microstructure and thermal/mechanical performance of fired porous samples was evaluated.

EXPERIMENTAL

Starting materials

Industrial grade mullite powder (d_{50} = 2.8 μm) was utilised as the main starting material, along with analytical grade $ZrSiO_4$ powder (98 %, d_{50} = 1 μm). Isobam-104 (*IB*) and sodium carboxymethyl cellulose (*CMC*) were chosen for dispersion/gelation and foam stabilization, respectively, and triethanolamine lauryl sulfate (*TLS*) was used for foaming.

Sample preparation

Mullite and 0 - 8 wt. % $ZrSiO_4$ were wet-mixed/homogenized in a ball mill. The wet mix was then oven-dried at 110 °C for overnight, and screened using a 100 mesh sieve. A slurry composed of 52 vol. % of the powder mix, 0.1 wt. % *CMC*, 0.5 wt. % *IB* and deionized water was prepared (2 min initial stirring, followed by immediate addition of 0.6 vol. % *TLS* and another 2 min further stirring). The foamed slurry was cast and cured in a mold. After demoulding, the samples were dried at 40 °C and 110 °C, for 2 days each, before being fired at 1400 °C for 2 h.

Sample characterization

A Malvern laser analyzer was used to measure particle size distribution. A Philips X-ray diffractometer (XRD) was used to identify crystalline phases in samples. ICDD cards used to assist phase analysis are mullite (01-079-1458) and $ZrSiO_4$ (74-1685). Porosity and density of samples were measured based on the Archimedes principle. Microstructure was observed by a scanning electronic microscope (SEM). Pore sizes were analyzed statistically on the basis of SEM images using the Micro-Images Analysis & Process System (MIAPS) package. Three-point bending strength and compressive strength were tested by using digitally controlled testers. Thermal conductivities at different temperatures (200 - 1000 °C) were examined using the water flow plate technique.

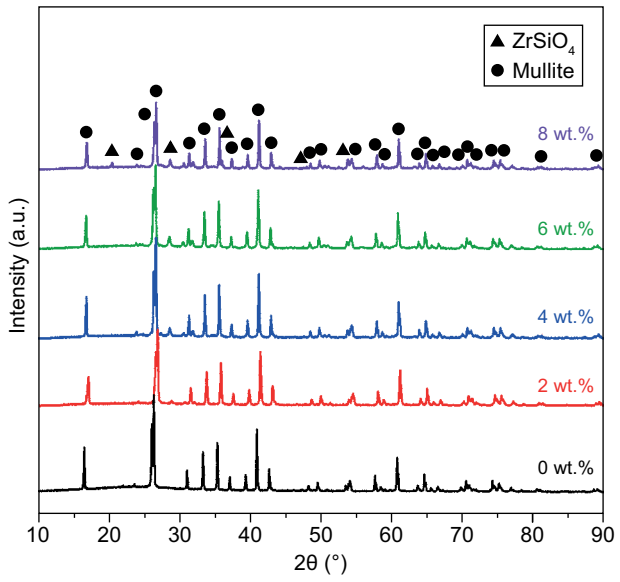

Figure 1. XRD patterns of samples containing various amounts of $ZrSiO_4$ after 2 h firing at 1400 °C.

RESULTS AND DISCUSSION

Figure 1 presents XRD results of samples with various contents of $ZrSiO_4$ fired for 2 h at 1400 °C. Mullite was identified as the main phase. Furthermore, in the $ZrSiO_4$ modified samples, as expected, $ZrSiO_4$ was present as the second phase, and its peak heights relative to those of mullite increased with its content. Except mullite and $ZrSiO_4$, no other phases were detected, indicating that on firing $ZrSiO_4$ neither reacted with mullite, nor decomposed to ZrO_2 and SiO_2. This was due to the lower firing temperature than the decomposition temperature of $ZrSiO_4$ [24].

Figure 2 illustrates SEM images of the samples after 2 h at 1400 °C, revealing a solid matrix and "large" spherical pores in the microstructure. High magnification images (on the right in Figure 2) further revealed the similarity in the overall microstructure and morphology of

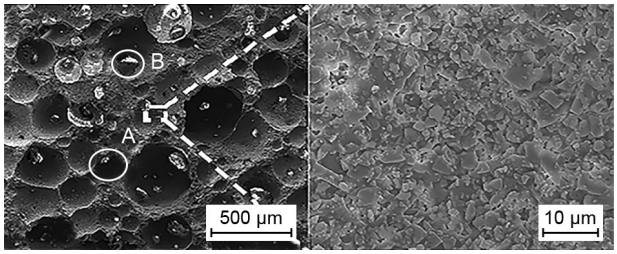

a) 0 wt. %

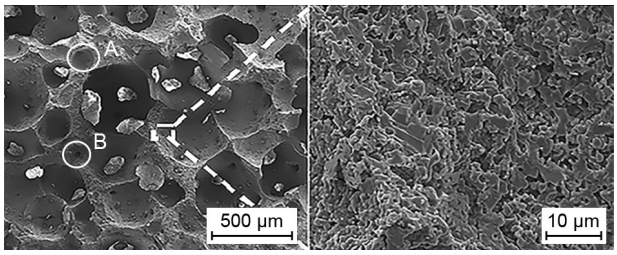

b) 2 wt. %

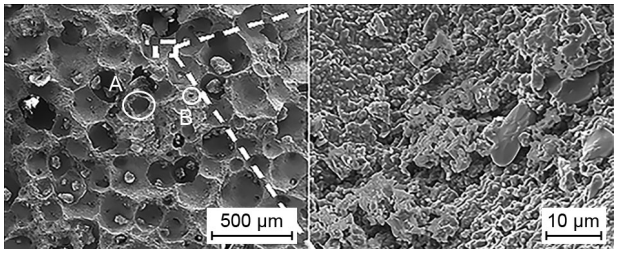

c) 4 wt. %

Figure 2. SEM images of samples with various contents of $ZrSiO_4$: a) 0 wt. %, b) 2 wt. %, c) 4 wt. %, after 2 h firing at 1400 °C. *(Continue on next page)*

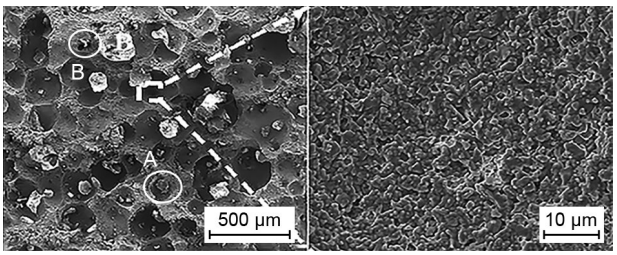

d) 6 wt. %

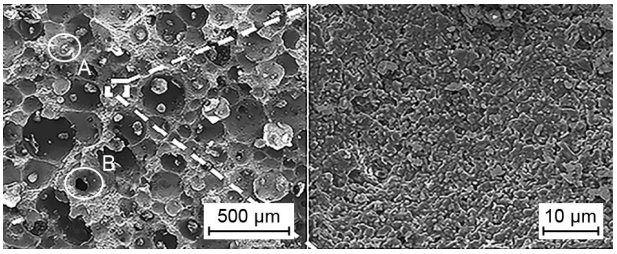

e) 8 wt. %

Figure 2. SEM images of samples with various contents of $ZrSiO_4$: d) 6 wt. %, e) 8 wt. %, after 2 h firing at 1400 °C.

the fired samples. The grains with similar shapes and sizes were distributed uniformly. Figure 2 also shows that the fired samples were all porous, containing relatively large spherical pores (highlighted by 'A'), and small window pores (highlighted by 'B') in internal walls of the former were generated. As discussed previously, their formation was related to the foaming, gas diffusion and sample sintering [20-22]. Moreover, it also can be seen from Figure 2 that when the $ZrSiO_4$ content rose from 0 to 8 wt. %, overall pore sizes in the fired samples appeared to become smaller and more homogeneous. According to the MIAPS analysis (Figure 3), as the $ZrSiO_4$ content increased from 0 to 8 wt. %, average size of the relatively large spherical pores (highlighted by 'A' in Figure 2) decreased from 171.0 to 141.9 μm (Figure 3).

Figure 4 demonstrates the influence of $ZrSiO_4$ content on the densification extent of samples heated at 1400 °C for 2 h. When the $ZrSiO_4$ content increased from 0 to 8 wt. %, the porosity and bulk density only varied within small ranges, 77 - 78 %, and 0.69 - 0.71 g·cm^3, respectively, indicating the little effect of $ZrSiO_4$ addition on the sample densification on firing. Nevertheless, in terms of the size-decrease of "large" spherical pores caused by the $ZrSiO_4$ addition (Figures 2 and 3), it can be considered that the $ZrSiO_4$ addition led to more centralized and homogeneous pore size distribution. In other words, $ZrSiO_4$ added to the mullite matrix led to a more uniform microstructure, which would impart better thermal performance to fired porous samples without compromising their high porosity and mechanical strength, which will be further discussed below.

Given in Figure 5 are flexural and compressive strengths of fired samples containing different amounts of $ZrSiO_4$, illustrating that both strengths were enhanced on increasing the $ZrSiO_4$ content from 0 to 6 wt. %, but began to decrease on further increasing the content from 6 to 8 wt. %. The highest flexural and compressive strengths corresponding to 6 wt. % of $ZrSiO_4$ addition were respectively 3.93 and 9.54 MPa. Although both

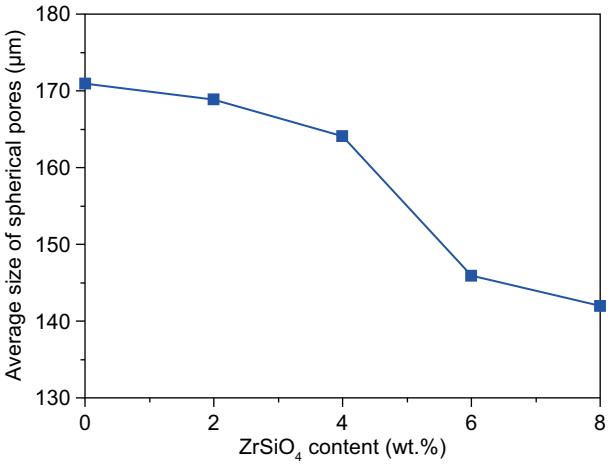

Figure 3. Effect of $ZrSiO_4$ content on the average size of "large" spherical pores in the samples fired at 1400 °C for 2 h.

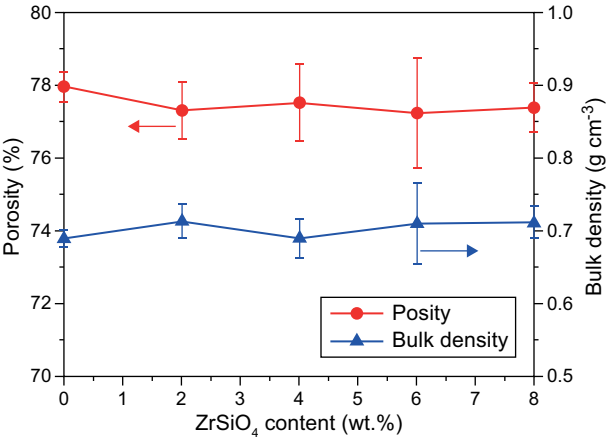

Figure 4. Porosity and bulk density of samples fired at 1400 °C for 2 h as a function of $ZrSiO_4$ content.

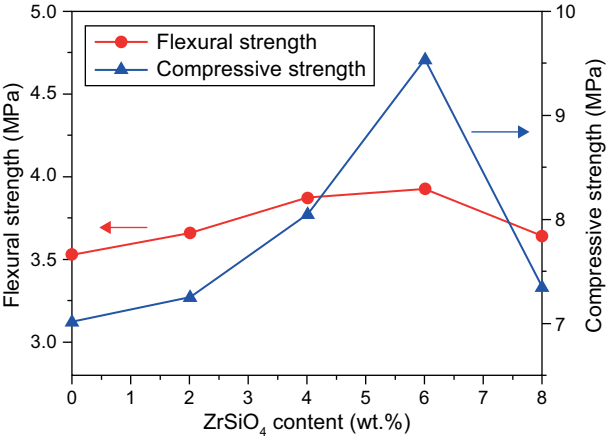

Figure 5. Effect of $ZrSiO_4$ content on mechanical strength of porous mullite samples fired at 1400 °C for 2 h.

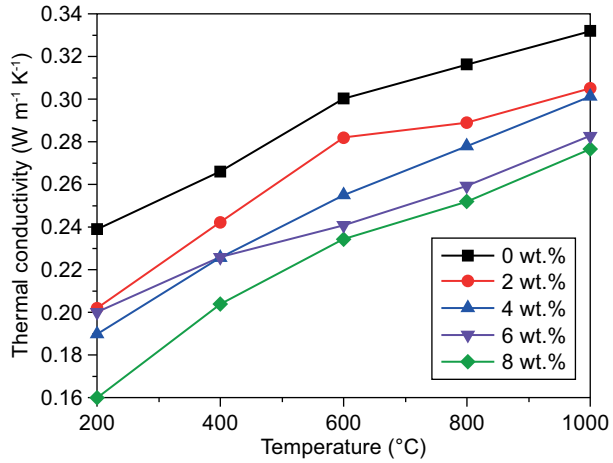

Figure 6. Thermal conductivity values of as-prepared samples containing various amounts of $ZrSiO_4$, at various testing temperatures.

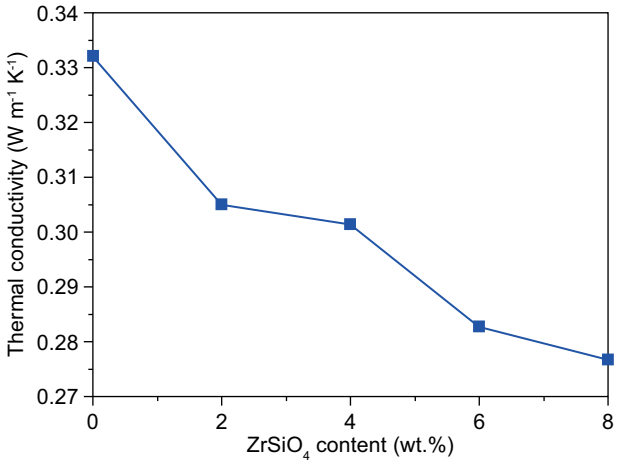

Figure 7. Thermal conductivity of as-prepared samples measured at 1000 °C as a function of $ZrSiO_4$ content.

strengths corresponding to 8 wt. % $ZrSiO_4$ addition decreased from their peak values, they were still higher than in the case of without $ZrSiO_4$ addition. These results indicated that the mechanical strength could be effectively enhanced by adding < 8 wt. % $ZrSiO_4$.

Thermal conductivities of fired samples were examined at various temperatures (200, 400, 600, 800 and 1000 °C) and are compared in Figure 6. For a given sample, its thermal conductivity increased with the test temperature. However, at a given test temperature, the thermal conductivity overall tended to decrease when the content of $ZrSiO_4$ was increased from 0 to 8 wt. %. For example, at 600 °C, it decreased to 0.234 $W \cdot m^{-1} \cdot K^{-1}$ as the $ZrSiO_4$ content rose to 8 wt. %. The lowest value (0.160 $W \cdot m^{-1} \cdot K^{-1}$) was seen in the case of the sample containing 8 wt. % $ZrSiO_4$ at 200 °C. The thermal conductivity of this sample at 1000 °C slightly increased to 0.277 $W \cdot m^{-1} \cdot K^{-1}$ but it was still very close to that of the sample without $ZrSiO_4$ at 200 °C. Considering the importance of thermal insulation at elevated temperature, the correlation of thermal conductivity at 1000 °C with the content of $ZrSiO_4$ is specifically demonstrated in Figure 7. As seen from Figure 7, the thermal conductivity at 1000 °C decreased as the $ZrSiO_4$ content rose from 0 to 8 wt. %, demonstrating further the beneficial effect of $ZrSiO_4$ addition for the thermal insulation even at high temperature. Comparison in Table 1 revealed that thermal conductivity values of as-prepared porous samples were competitive with those reported previously for their porous counterparts prepared *via* other routes, suggesting that foam-gelcating combined with $ZrSiO_4$ addition was feasible to make mullite based porous ceramics with good insulation performance, especially at an elevated temperature.

Table 1. Comparison of thermal conductivity of as-prepared porous mullite with the data reported in literature.

Method	Porosity (%)	Test temperature and measure method	Thermal conductivity ($W \cdot m^{-1} \cdot K^{-1}$)	Reference
Gel-casting	71.7	25 °C, laser flash method	0.378	[7]
Foaming	65.32 - 83.02	1100 °C, flat plate method	0.28 - 0.42	[15]
Foam-gelcasting and microwave heating	76.6	25 °C, hot disk method	0.269	[18]
Foam-gelcasting combined with pore-forming agent	79.1	200 °C, standard water flow plate method	0.11	[19]
Foaming and starch consolidation	~ 76.2	25 °C, hot disk method	~ 0.31	[28]
Foam-gelcasting with $ZrSiO_4$ addition	77.4	200 °C, standard water flow plate method	0.160	Present work
		1000 °C, standard water flow plate method	0.277	

The thermal conductivity of dense mullite is slightly lower than that of dense $ZrSiO_4$ [25]. Despite small amounts of addition, the added $ZrSiO_4$ should still result in enhanced thermal conductivity, however, the test results showed the opposite, which can be explained by the roles played by the added $ZrSiO_4$. On the one hand, it acted as an IR opacifer, blocking the IR radiation *via* shading effect, and thus reducing the overall heat transfer. On the other hand, it might also assist reducing the thermal conductivity *via* decreasing the average size of "large" spherical pores and narrowing distribution of pore size. In terms of literature, at a given level of porosity, thermal conductivity decreases when the pore size decreases. According to Nait-Ali *et al.*, to fabricate an effective thermal insulation material, it was necessary to form high volume fraction of small pores in the microstructure [26]. Furthermore, Alvarez *et al.* considered that pore radius played a relevant role in the thermal conductivity reduction [27]. In addition, at a high operating temperature, the heat radiation would become more significant than the conduction and the convection. Thermal conductivity of a porous ceramic *via* radiation was positively related to the maximum pore size [15]. As shown in Figures 2 and 3, the $ZrSiO_4$ addition led to the decrease in the overall size of "large" pores, thus further decreasing the high temperature thermal conductivity of fired porous samples.

Several factors can affect thermal property of a porous material. As well known, thermal conductivity decreases with an increase in the porosity. Apart from this, the microstructure could make a great difference [28]. Isotropic porous materials can be classified into two types: internal porosity material and external porosity material [29]. Based on the thermal conductivity at 200 °C (Figure 6), the porous samples prepared in this work exhibited similar characteristics to those of internal porosity materials [28, 29]. For such materials, heat is transferred mainly through their matrix which is more thermally conductive, and their effective thermal conductivity is bounded above that predicted by the Maxwell-Eucken model but below that predicted by the EMT model [28].

CONCLUSIONS

Mullite based porous ceramics were fabricated by using a foam gelcasting method. Isobam-104, CMC, and TLS were used respectively as dispersing/gelling, foam stabilizing, and foaming agents. The fired porous mullite sample containing 8 wt. % $ZrSiO_4$ showed high porosity up to 77.4 %, high compressive strength up to 7.35 MPa, and low thermal conductivity: 0.160 and 0.277 $W \cdot m^{-1} \cdot K^{-1}$ at 200 and 1000 °C, respectively. The addition of $ZrSiO_4$ was beneficial for effective reduction of thermal conductivity, in particular at a high temperature.

Acknowledgments

The authors would like to acknowledge the financial support from The State Key Laboratory of Refractories and Metallurgy (Wuhan University of Science and Technology), No. G201810; National Natural Science Foundation of China (Grant No.51672194); Natural Science Foundation of Jiangxi Province, China, Contract No. 20181BAB216006; Program for Innovative Teams of Outstanding Young and Middle-aged Researchers in the Higher Education Institutions of Hubei Province (T201602); Key Program of Natural Science Foundation of Hubei Province, China (Contract No. 2017CFA004) and the Doctoral Scientific Research Foundation of Quzhou University (Grant no. BSYJ201707).

REFERENCES

1. Barea R., Osendi M. I., Miranzo P., Ferreira J. M. F. (2005): Fabrication of Highly Porous Mullite Materials, *Journal of the American Ceramic Society*, 88 (3), 777-779. doi: 10.1111/j.1551-2916.2005.00092.x
2. She J. H., Ohji T. (2003): Fabrication and characterization of highly porous mullite ceramics, *Materials Chemistry and Physics*, 80 (3), 610-614. doi: 10.1016/S0254-0584 (03)00080-4
3. Chen M., Zhu L., Dong Y., Li L., Liu J. (2016): Waste-to-Resource Strategy To Fabricate Highly Porous Whisker-Structured Mullite Ceramic Membrane for Simulated Oil-in-Water Emulsion Wastewater Treatment, *ACS Sustainable Chemistry & Engineering*, 4 (4), 2098-2106. doi: 10.1021/acssuschemeng.5b01519
4. Liu R., Zhang F., Su W., Zhao H., Wang C.-A. (2015): Impregnation of porous mullite with Na_2SO_4 phase change material for thermal energy storage, *Solar Energy Materials and Solar Cells*, 134, 268-274. doi: 10.1016/j.solmat.2014.12.012
5. Ahmad R., Anwar M. S., Kim J., Song I.-H., Abbas S. Z., Ali S. A., Ali F., Ahmad J., Bin Awais H., Mehmood M. (2016): Porosity features and gas permeability analysis of bi-modal porous alumina and mullite for filtration applications, *Ceramics International*, 42 (16), 18711-18717. doi: 10.1016/j.ceramint.2016.09.009
6. Kim Y.-W., HKim.-D., Park C. B. (2005): Processing of Microcellular Mullite, *Journal of the American Ceramic Society*, 88 (12), 3311-3315. doi: 10.1111/j.1551-2916.2005.00597.x
7. Yuan L., Ma B., Zhu Q., Zhang X., Zhang H., Yu J. (2017): Preparation and properties of mullite-bonded porous fibrous mullite ceramics by an epoxy resin gel-casting process, *Ceramics International*, 43 (7), 5478-5483. doi: 10.1016/j.ceramint.2017.01.062
8. Hou Z., Du H., Liu J., Hao R., Dong X., Liu M. (2013): Fabrication and properties of mullite fiber matrix porous ceramics by a TBA-based gel-casting process, *Journal of the European Ceramic Society*, 33 (4), 717-725. doi: 10.1016/j.jeurceramsoc.2012.10.011
9. Luo H., Li Y. B., Li S. J., Chen R. Y., Xiang R. F., Xu N. N., Wang Q. H., Si O. Y. (2018): Fabrication of Porous Mullite Ceramics with Different Phase of Alumina for Insulation

Materials, *Solid State Phenomena*, 281, 242-248. doi: 10.4028/www.scientific.net/SSP.281.242

10. Li N., Zhang X.-Y., Qu Y.-N., Xu J., Ma N., Gan K., Huo W.-L., Yang J.-L. (2016): A simple and efficient way to prepare porous mullite matrix ceramics via directly sintering SiO_2-Al_2O_3 microspheres, *Journal of the European Ceramic Society*, 36 (11), 2807-2812. doi: 10.1016/j.jeurceramsoc.2016.03.037
11. Barea R., Osendi M. I., Ferreira J. M. F., Miranzo P. (2005): Thermal conductivity of highly porous mullite material, *Acta Materialia*, 53 (11), 3313-3318. doi: 10.1016/j.actamat.2005.03.040
12. Zhang B., Ma J., Ye J., Jin Y., Yang C., Ding J., Zhang Z., Hou Z., Liu Q., Ye F. (2019): Ultra-low cost porous mullite ceramics with excellent dielectric properties and low thermal conductivity fabricated from kaolin for radome applications, *Ceramics International*. doi: 10.1016/j.ceramint.2019.06.120
13. Deng X., Wang J., Liu J., Zhang H., Li F., Duan H., Lu L., Huang Z., Zhao W., Zhang S. (2015): Preparation and characterization of porous mullite ceramics via foam-gelcasting, *Ceramics International*, 41 (7), 9009-9017. doi: 10.1016/j.ceramint.2015.03.237
14. Li C., Bian C., Han Y., Wang C.-A., An L. (2016): Mullite whisker reinforced porous anorthite ceramics with low thermal conductivity and high strength, *Journal of the European Ceramic Society*, 36 (3), 761-765. doi: 10.1016/j.jeurceramsoc.2015.10.002
15. Guo H., Li W., Ye F. (2016): Preparation of microporous mullite ceramics by foaming for high temperature thermal isolation, *Ceramics International*, 42 (15), 17332-17338. doi: 10.1016/j.ceramint.2016.08.029
16. Deng X., Ran S., Han L., Zhang H., Ge S., Zhang S. (2017): Foam-gelcasting preparation of high-strength self-reinforced porous mullite ceramics, *Journal of the European Ceramic Society*, 37 (13), 4059-4066. doi: 10.1016/j.jeurceramsoc.2017.05.009
17. Deng X., Wu Y., Wei T., Ran S., Huang L., Zhang H., Li F., Han L., Ge S., Zhang S. (2018): Preparation of elongated mullite self-reinforced porous ceramics, *Ceramics International*, 44 (7), 7500-7508. doi: 10.1016/j.ceramint.2018.01.144
18. Han L., Deng X., Li F., Huang L., Pei Y., Dong L., Li S., Jia Q., Zhang H., Zhang S. (2018): Preparation of high strength porous mullite ceramics via combined foam-gelcasting and microwave heating, *Ceramics International*, 44 (12), 14728-14733. doi: 10.1016/j.ceramint.2018.05.101
19. Ge S., Lin L., Zhang H., Bi Y., Zheng Y., Li J., Deng X., Zhang S. (2018): Synthesis of hierarchically porous mullite ceramics with improved thermal insulation via foam-gelcasting combined with pore former addition, *Advances in Applied Ceramics*, 117 (8), 493-499. doi: 10.1080/17436753.2018.1502065
20. Han L., Li F., Deng X., Wang J., Zhang H., Zhang S. (2017): Foam-gelcasting preparation, microstructure and thermal insulation performance of porous diatomite ceramics with hierarchical pore structures, *Journal of the European Ceramic Society*, 37 (7), 2717-2725. doi: doi:10.1016/j.jeurceramsoc.2017.02.032
21. Zhang B.-M., Zhao S.-Y., He X.-D. (2008): Experimental and theoretical studies on high-temperature thermal properties of fibrous insulation, *Journal of Quantitative Spectroscopy and Radiative Transfer*, 109 (7), 1309-1324. doi: 10.1016/j.jqsrt.2007.10.008
22. Feng J., Chen D., Ni W., Yang S., Hu Z. (2010): Study of IR absorption properties of fumed silica-opacifier composites, *Journal of Non-Crystalline Solids*, 356 (9), 480-483. doi: 10.1016/j.jnoncrysol.2009.12.015
23. Lu G., Wang X.-D., Duan Y.-Y., Li X.-W. (2011): Effects of non-ideal structures and high temperatures on the insulation properties of aerogel-based composite materials, *Journal of Non-Crystalline Solids*, 357 (22), 3822-3829. doi: 10.1016/j.jnoncrysol.2011.07.022
24. Zhao S.-K., Huang Y., Wang C.-A., Huang X.-X., Guo J.-K. (2003): Mullite formation from reaction sintering of $ZrSiO_4$/α-Al_2O_3 mixtures, *Materials Letters*, 57 (11), 1716-1722. doi: 10.1016/S0167-577X(02)01057-1
25. Nakamori F., Ohishi Y., Muta H., Kurosaki K., Fukumoto K., Yamanaka S. (2017): Mechanical and thermal properties of $ZrSiO_4$, *Journal of Nuclear Science & Technology*, 54 (11), 1-7.
26. Nait-Ali B., Haberko K., Vesteghem H., Absi J., Smith D. S. (2006): Thermal conductivity of highly porous zirconia, *Journal of the European Ceramic Society*, 26 (16), 3567-3574. doi: 10.1016/j.jeurceramsoc.2005.11.011
27. Alvarez F. X., Jou D., Sellitto A. (2010): Pore-size dependence of the thermal conductivity of porous silicon: A phonon hydrodynamic approach, *Applied Physics Letters*, 97 (3), 033103. doi: 10.1063/1.3462936
28. Gong L., Wang Y., Cheng X., Zhang R., Zhang H. (2013): Thermal conductivity of highly porous mullite materials, *International Journal of Heat and Mass Transfer*, 67, 253-259. doi: 10.1016/j.ijheatmasstransfer.2013.08.008
29. Carson J. K., Lovatt S. J., Tanner D. J., Cleland A. C. (2005): Thermal conductivity bounds for isotropic, porous materials, *International Journal of Heat and Mass Transfer*, 48 (11), 2150-2158. doi: 10.1016/j.ijheatmasstransfer.2004.12.032